Physics Letters B 750 (2015) 53–58

Contents lists available at ScienceDirect

Physics Letters B

www.elsevier.com/locate/physletb

First measurement of the polarization observable E in the $\vec{p}(\vec{\gamma},\pi^+)n$ reaction up to 2.25 GeV

CLAS Collaboration

S. Strauch [ai,*], W.J. Briscoe [m], M. Döring [m], E. Klempt [ag], V.A. Nikonov [ag,z], E. Pasyuk [ak], D. Rönchen [ag], A.V. Sarantsev [ag,z], I. Strakovsky [m], R. Workman [m], K.P. Adhikari [ad], D. Adikaram [ad], M.D. Anderson [an], S. Anefalos Pereira [p], A.V. Anisovich [ag,z], R.A. Badui [j], J. Ball [g], V. Batourine [ak], M. Battaglieri [q], I. Bedlinskiy [u], N. Benmouna [y], A.S. Biselli [i], J. Brock [ak], W.K. Brooks [al,ak], V.D. Burkert [ak], T. Cao [ai], C. Carlin [ak], D.S. Carman [ak], A. Celentano [q], S. Chandavar [ac], G. Charles [t], L. Colaneri [r,af], P.L. Cole [n], N. Compton [ac], M. Contalbrigo [o], O. Cortes [n], V. Crede [k], N. Dashyan [ar], A. D'Angelo [r,af], R. De Vita [q], E. De Sanctis [p], A. Deur [ak], C. Djalali [ai], M. Dugger [b], R. Dupre [t], H. Egiyan [ak,aa], A. El Alaoui [al], L. El Fassi [ad,a], L. Elouadrhiri [ak], P. Eugenio [k], G. Fedotov [ai,ah], S. Fegan [q], A. Filippi [s], J.A. Fleming [am], T.A. Forest [n], A. Fradi [t], N. Gevorgyan [ar], Y. Ghandilyan [ar], K.L. Giovanetti [v], F.X. Girod [ak,g], D.I. Glazier [an], W. Gohn [h,1], E. Golovatch [ah], R.W. Gothe [ai], K.A. Griffioen [aq], M. Guidal [t], L. Guo [j,ak], K. Hafidi [a], H. Hakobyan [al,ar], C. Hanretty [ak], N. Harrison [h], M. Hattawy [t], K. Hicks [ac], D. Ho [e], M. Holtrop [aa], S.M. Hughes [am], Y. Ilieva [ai,m], D.G. Ireland [an], B.S. Ishkhanov [ah], E.L. Isupov [ah], D. Jenkins [ao], H. Jiang [ai], H.S. Jo [t], K. Joo [h], S. Joosten [aj], C.D. Keith [ak], D. Keller [ap], G. Khachatryan [ar], M. Khandaker [n,ab], A. Kim [h], W. Kim [w], A. Klein [ad], F.J. Klein [f], V. Kubarovsky [ak], S.E. Kuhn [ad], P. Lenisa [o], K. Livingston [an], H.Y. Lu [ai], I.J.D. MacGregor [an], N. Markov [h], B. McKinnon [an], D.G. Meekins [ak], C.A. Meyer [e], V. Mokeev [ak,ah], R.A. Montgomery [p], C.I. Moody [a], H. Moutarde [g], A. Movsisyan [o], E. Munevar [ak,m], C. Munoz Camacho [t], P. Nadel-Turonski [ak,f,m], L.A. Net [ai], S. Niccolai [t], G. Niculescu [v], I. Niculescu [v], G. O'Rielly [x], M. Osipenko [q], A.I. Ostrovidov [k], K. Park [ak,ai,w,2], P. Peng [ap], W. Phelps [j], J.J. Phillips [an], S. Pisano [p], O. Pogorelko [u], S. Pozdniakov [u], J.W. Price [c], S. Procureur [g], Y. Prok [ad,ap], D. Protopopescu [an], A.J.R. Puckett [h], B.A. Raue [j,ak], M. Ripani [q], B.G. Ritchie [b], A. Rizzo [r,af], G. Rosner [an], P. Roy [k], F. Sabatié [g], C. Salgado [ab], D. Schott [m,j], R.A. Schumacher [e], E. Seder [h], M.L. Seely [ak], I. Senderovich [b], Y.G. Sharabian [ak], A. Simonyan [ar], Iu. Skorodumina [ai,ah], G.D. Smith [am], D.I. Sober [f], D. Sokhan [an,am], N. Sparveris [aj], P. Stoler [ae], S. Stepanyan [ak], V. Sytnik [al], M. Taiuti [l,3], Ye Tian [ai], A. Trivedi [ai], R. Tucker [b], M. Ungaro [ak,h], H. Voskanyan [ar], E. Voutier [t], N.K. Walford [f], D.P. Watts [am], X. Wei [ak], M.H. Wood [d,ai], N. Zachariou [ai], L. Zana [am,aa], J. Zhang [ak,ad], Z.W. Zhao [ad,ai,ak], I. Zonta [r,af]

[a] *Argonne National Laboratory, Argonne, IL 60439, USA*
[b] *Arizona State University, Tempe, AZ 85287-1504, USA*

* Corresponding author.
E-mail address: strauch@sc.edu (S. Strauch).
[1] Current address: University of Kentucky, Lexington, Kentucky 40506.
[2] Current address: Old Dominion University, Norfolk, Virginia 23529.
[3] Current address: INFN, Sezione di Genova, 16146 Genova, Italy.

http://dx.doi.org/10.1016/j.physletb.2015.08.053

[c] California State University, Dominguez Hills, Carson, CA 90747, USA
[d] Canisius College, Buffalo, NY, USA
[e] Carnegie Mellon University, Pittsburgh, PA 15213, USA
[f] Catholic University of America, Washington DC 20064, USA
[g] CEA, Centre de Saclay, Irfu/Service de Physique Nucléaire, 91191 Gif-sur-Yvette, France
[h] University of Connecticut, Storrs, CT 06269, USA
[i] Fairfield University, Fairfield, CT 06824, USA
[j] Florida International University, Miami, FL 33199, USA
[k] Florida State University, Tallahassee, FL 32306, USA
[l] Università di Genova, 16146 Genova, Italy
[m] The George Washington University, Washington, DC 20052, USA
[n] Idaho State University, Pocatello, ID 83209, USA
[o] INFN, Sezione di Ferrara, 44100 Ferrara, Italy
[p] INFN, Laboratori Nazionali di Frascati, 00044 Frascati, Italy
[q] INFN, Sezione di Genova, 16146 Genova, Italy
[r] INFN, Sezione di Roma Tor Vergata, 00133 Rome, Italy
[s] INFN, Sezione di Torino, 10125 Torino, Italy
[t] Institut de Physique Nucléaire, CNRS/IN2P3 and Université Paris Sud, Orsay, France
[u] Institute of Theoretical and Experimental Physics, Moscow, 117259, Russia
[v] James Madison University, Harrisonburg, VA 22807, USA
[w] Kyungpook National University, Daegu 702-701, Republic of Korea
[x] University of Massachusetts Dartmouth, Dartmouth, MA 02747, USA
[y] Montgomery College, Rockville, MD 20850, USA
[z] NRC "Kurchatov Institute", PNPI, 188300, Gatchina, Russia
[aa] University of New Hampshire, Durham, NH 03824-3568, USA
[ab] Norfolk State University, Norfolk, VA 23504, USA
[ac] Ohio University, Athens, OH 45701, USA
[ad] Old Dominion University, Norfolk, VA 23529, USA
[ae] Rensselaer Polytechnic Institute, Troy, NY 12180-3590, USA
[af] Università di Roma Tor Vergata, 00133 Rome, Italy
[ag] Universität Bonn, 53115 Bonn, Germany
[ah] Skobeltsyn Institute of Nuclear Physics, Lomonosov Moscow State University, 119234 Moscow, Russia
[ai] University of South Carolina, Columbia, SC 29208, USA
[aj] Temple University, Philadelphia, PA 19122, USA
[ak] Thomas Jefferson National Accelerator Facility, Newport News, VA 23606, USA
[al] Universidad Técnica Federico Santa María, Casilla 110-V Valparaíso, Chile
[am] Edinburgh University, Edinburgh EH9 3JZ, United Kingdom
[an] University of Glasgow, Glasgow G12 8QQ, United Kingdom
[ao] Virginia Tech, Blacksburg, VA 24061-0435, USA
[ap] University of Virginia, Charlottesville, VA 22901, USA
[aq] College of William and Mary, Williamsburg, VA 23187-8795, USA
[ar] Yerevan Physics Institute, 375036 Yerevan, Armenia

ARTICLE INFO

Article history:
Received 7 June 2015
Received in revised form 21 August 2015
Accepted 23 August 2015
Available online 28 August 2015
Editor: D.F. Geesaman

Keywords:
Baryon spectroscopy
Pion photoproduction
Polarization observables
FROST experiment

ABSTRACT

First results from the longitudinally polarized frozen-spin target (FROST) program are reported. The double-polarization observable E, for the reaction $\vec{\gamma}\vec{p} \to \pi^+ n$, has been measured using a circularly polarized tagged-photon beam, with energies from 0.35 to 2.37 GeV. The final-state pions were detected with the CEBAF Large Acceptance Spectrometer in Hall B at the Thomas Jefferson National Accelerator Facility. These polarization data agree fairly well with previous partial-wave analyses at low photon energies. Over much of the covered energy range, however, significant deviations are observed, particularly in the high-energy region where high-L multipoles contribute. The data have been included in new multipole analyses resulting in updated nucleon resonance parameters. We report updated fits from the Bonn–Gatchina, Jülich–Bonn, and SAID groups.

The spectrum of baryon resonances strongly depends on the internal dynamics of its underlying constituents. Recent lattice calculations and quark models reveal a rich spectrum, in contrast to phenomenological analyses of experiments, which have found a smaller number of states [1,2]. The so-called missing resonances have stimulated alternative interpretations of the resonance spectrum. These include the formation of quasi-stable diquarks [3], string models running under the acronym AdS/QCD [4], models assuming some baryon resonances are dynamically generated from the unitarized interaction among ground-state baryons and mesons [5], and the speculation that a phase transition may occur in high-mass excitations [6]. The photoproduction of mesons off nucleons provides an opportunity to distinguish among these alternatives.

Four complex amplitudes govern the photoproduction of single pions, and a *complete* experiment requires the measurement of at least eight well-chosen observables at each energy and production angle for both isospin-related reactions $\gamma p \to \pi^0 p$ and $\gamma p \to \pi^+ n$ [7]. However, the current database for pion photoproduction is populated mainly by unpolarized cross sections and single-spin observables, which do not form a complete experiment. This is particularly true for $\pi^+ n$ photoproduction at photon energies above 1.8 GeV. This incompleteness of the database leads to ambiguities in the multipole solutions.

In this Letter we present a measurement of the double-polarization observable E in the $\vec{\gamma}\vec{p} \to \pi^+ n$ reaction of circularly polarized photons with longitudinally polarized protons. The polarized cross section is in this case given by [8]

$$\left(\frac{d\sigma}{d\Omega}\right) = \left(\frac{d\sigma}{d\Omega}\right)_0 (1 - P_z P_\odot E)\,, \tag{1}$$

where $(d\sigma/d\Omega)_0$ is the unpolarized cross section; P_z and $P_\odot$ are the target and beam polarizations, respectively. The observable E is the helicity asymmetry of the cross section,

$$E = \frac{d\sigma_{1/2} - d\sigma_{3/2}}{d\sigma_{1/2} + d\sigma_{3/2}} \tag{2}$$

for aligned, total helicity $h = 3/2$, and anti-aligned, $h = 1/2$, photon and proton spins. These data are fitted using three very different PWA models — BnGa, JüBo, and SAID — from the Bonn–Gatchina [9], Jülich–Bonn [10], and GWU [11] groups, respectively. The resulting consistency of helicity amplitudes for the dominant resonances demonstrates that the PWA results are largely driven by the data alone; the modest differences gauge the model-dependence. This consistency provides an excellent starting point to search for new resonances.

Earlier measurements have been reported for the polarization observable E in the $\pi^0 p$ channel [12] and some cross-section helicity-asymmetry data exists for both the $\pi^0 p$ and $\pi^+ n$ channels [13–15]. Here we report E measurements of unprecedented precision covering, for the first time, nearly the entire resonance region.

The experiment was performed at the Thomas Jefferson National Accelerator Facility (JLab). Longitudinally polarized electrons from the CEBAF accelerator with energies of $E_e = 1.645$ GeV and 2.478 GeV were incident on the thin radiator of the Hall-B Photon Tagger [16] and produced circularly polarized tagged photons in the energy range between $E_\gamma = 0.35$ GeV and 2.37 GeV.

The degree of circular polarization of the photon beam, $P_\odot$, depends on the ratio $x = E_\gamma/E_e$ and increases from zero to the degree of incident electron-beam polarization, P_e, monotonically with photon energy [17]

$$P_\odot = P_e \cdot \frac{4x - x^2}{4 - 4x + 3x^2}. \tag{3}$$

Measurements of the electron-beam polarization were made routinely with the Hall-B Møller polarimeter. The average value of the electron-beam polarization was found to be $P_e = 0.84 \pm 0.04$. The electron-beam helicity was pseudo-randomly flipped between $+1$ and -1 with a 30 Hz flip rate.

The collimated photon beam irradiated a frozen-spin target (FROST) [18] at the center of the CEBAF Large Acceptance Spectrometer (CLAS) [19]. Frozen beads of butanol (C_4H_9OH) inside a 50 mm long target cup were used as target material. The protons of the hydrogen atoms in this material were dynamically polarized along the photon-beam direction. The degree of polarization was on average $P_z = 0.82 \pm 0.05$. The proton polarization was routinely changed from being aligned along the beam axis to being anti-aligned. Quasi-free photoproduction off the unpolarized, bound protons in the butanol target constituted a background. Data were taken simultaneously from an additional carbon target downstream of the butanol target to allow for the determination of this bound-nucleon background. A small unpolarized hydrogen contamination of the carbon target has been corrected for in the analysis.

Final-state π^+ mesons were detected in CLAS. The particle detectors used in this experiment were a set of plastic scintillation counters close to the target to measure event start times (start counter) [20], drift chambers [21] to determine charged-particle trajectories in the magnetic field within CLAS, and scintillation counters for flight-time measurements [22]. Coincident signals from the photon tagger, start-, and time-of-flight counters constituted the event trigger. Data from this experiment were taken in seven groups of runs with various electron-beam energies and beam/target polarization orientations. Events with one and only one positively charged particle and zero negatively charged particles detected in CLAS were considered. The π^+ mesons were identified by their charge (from the curvature of the particle track) and by using the time-of-flight technique. Photoproduced lepton-pair production in the nuclear targets was a forward peaked background. This background was strongly suppressed with a fiducial cut on the polar angle of the pion, $\theta_\pi^{\rm lab} > 14^\circ$.

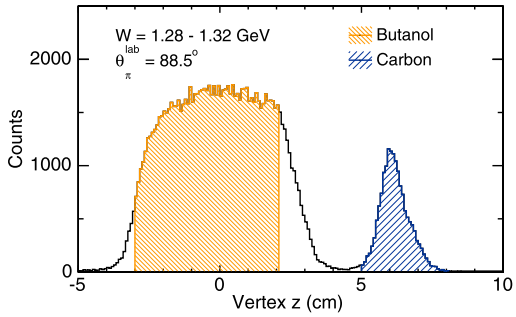

Fig. 1. Example of a reconstructed distribution of the reaction vertex along the beam line for events at $W \approx 1.30$ GeV and $\theta^{\rm lab} \approx 88.5^\circ$ originating in the butanol and carbon targets. The shaded areas indicate the z-vertex ranges used in the analysis.

The observable E was determined in 900 kinematic bins of W and $\cos\theta_\pi^{\rm cm}$, where W is the center-of-mass energy and $\theta_\pi^{\rm cm}$ is the pion center-of-mass angle with respect to the incident photon momentum direction. For each bin three missing-mass distributions in the $\gamma p \to \pi^+ X$ reaction were accumulated: for events originating in the butanol-target with a total helicity of photons and polarized protons of $h = 3/2$, for butanol events with $h = 1/2$, and for events originating in the carbon-target. The production target was identified by the reconstructed position of the reaction vertex; see Fig. 1. The range for butanol-target events, -3 cm to $+2$ cm, was selected to maximize their yield while minimizing potential contributions from unpolarized events. To determine the bound-nucleon background in the butanol data, the carbon-data distribution was scaled by a factor α to fit the butanol missing-mass distribution up to 1.05 GeV/c^2, together with a Gaussian peak. Over all kinematic bins, the average value of α is 5. Examples of two angular bins at $W \approx 1.63$ GeV are shown in Fig. 2. The number of events, $N^B_{3/2}$, $N^B_{1/2}$, and N^C, for a given kinematic bin were then selected by the condition $|m_X - m_0| < 2\sigma_H$, where m_0 and σ_H are the peak position and peak width of the neutron in the missing mass distribution taken from the fit. The selection is indicated by the hatched region in Fig. 2.

The observable E was finally extracted from the polarized yields, $N^p_{3/2}$ and $N^p_{1/2}$, of $\vec{\gamma}\vec{p} \to \pi^+ n$ events for total helicities $h = 3/2$ and $1/2$, respectively, and the average beam and target polarizations,

$$E = \frac{1}{\overline{P}_z \overline{P}_\odot} \left(\frac{N^p_{1/2} - N^p_{3/2}}{N^p_{1/2} + N^p_{3/2}}\right). \tag{4}$$

As the bound nucleons in the butanol target are unpolarized, the helicity difference in the event numbers is due only to the polarized hydrogen, $N^p_{1/2} - N^p_{3/2} = N^B_{1/2} - N^B_{3/2}$. The total yield from polarized hydrogen was determined from the butanol and carbon yields, $N^p_{1/2} + N^p_{3/2} = (N^B_{1/2} + N^B_{3/2} - \alpha N^C)\kappa$, where $\kappa = 1.3$ is an experimentally well determined correction factor. The correction is needed as N^C not only counts bound-nucleon events but also unpolarized free-proton events due to the hydrogen contamination of the carbon target. This is the largest contribution to κ and it is energy and scattering-angle independent. A minor contribution to κ arises as N^B and N^C contain also carbon-target and butanol-target

events, respectively, due to the limited resolution in the target reconstruction at very forward pion angles. The experimental value for E is then given by

$$E = \frac{1}{\overline{P}_z \overline{P}_\odot \kappa} \left[\frac{N^B_{1/2} - N^B_{3/2}}{N^B_{1/2} + N^B_{3/2} - \alpha N^C} \right]. \quad (5)$$

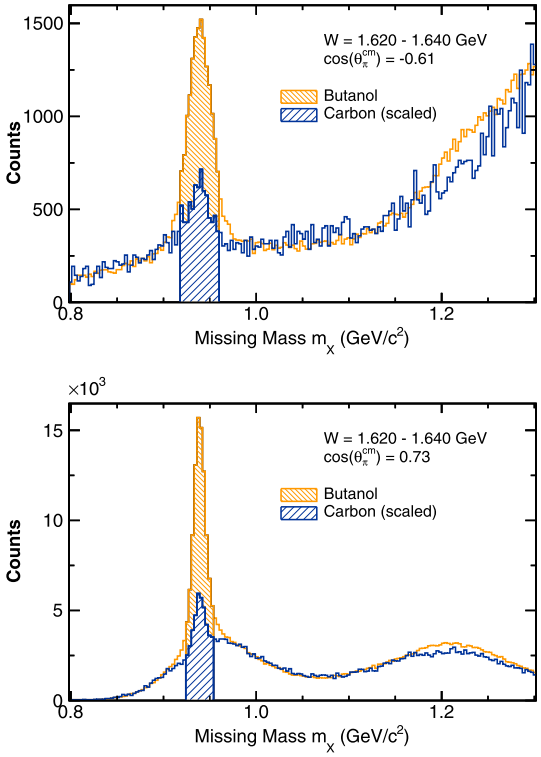

Fig. 2. (Color online.) Examples of butanol missing-mass distributions, $\gamma p \to \pi^+ X$, overlaid with scaled distributions from the carbon-target. The hatched region selects the butanol- and carbon-target events which were used in the subsequent analysis. The butanol yield at larger missing masses contains multi-pion final-state events off the free proton and exceed the carbon yield.

The statistical uncertainty of E is determined from the counting statistics of the event yields and from the statistical uncertainty of the scale factor α. The relative systematic uncertainty is dominated by the uncertainty in the product of the beam and target polarizations, about $\pm 7.5\%$. The hydrogen contamination contributes with $\pm 1.5\%$. Point-to-point uncertainties are due to the background subtraction, ± 0.03, and, only at the most forward pion angles, due to the limited vertex resolution, an additional contribution < 0.015.

The angular distributions, plotted in Fig. 3 as functions of $\cos\theta_\pi^{\rm cm}$, display an approximate 'U'-shaped distribution between the required maxima at $\cos\theta_\pi^{\rm cm} = \pm 1$ and dipping to about -0.5 for energies up to about $W = 1.7$ GeV. This differs from the E measurements for $\pi^0 p$ photoproduction from CBELSA-TAPS [12]. There, in a broad energy bin covering 960–1100 MeV, one sees a zero crossing near 90 degrees. In general, for the $\pi^+ n$ final state and $W < 1.5$ GeV, the data are well described [9–11], as Fig. 3 shows, because the analyses are constrained by older MAMI–B data [15]. However, at most of the higher photon energies, where no similar constraints exist, the BnGa, JüBo, and SAID analyses show more pronounced angular variations than are seen in the data. These qualitative features exist in the MAID [23] results as well.

Given the relative lack of polarization data at the highest energies, it is not surprising that a much better fit to these new E measurements is achieved once they are included in the database. These improved analyses maintain nevertheless good descriptions of the previous data. In principle, a fit may be achieved through small amplitude changes that produce large changes in the polarization observables, through a substantial modification of the assumed resonance and background contributions, or through the addition of new resonances. Having the BnGa, JüBo and SAID analyses together we are able to compare results with a minimal set of resonances (SAID) to the larger sets required in the BnGa and JüBo analyses.

To show the impact of the new E data, Table 1 shows the helicity couplings of selected low-mass nucleon resonances before and after including the data in the three analyses. The baseline SAID and JüBo fits were done with the same updated database to have a common point of comparison. The SAID and BnGa analyses compare changes in the Breit–Wigner resonance photo-decay parameters, while the JüBo results determine photo-couplings at

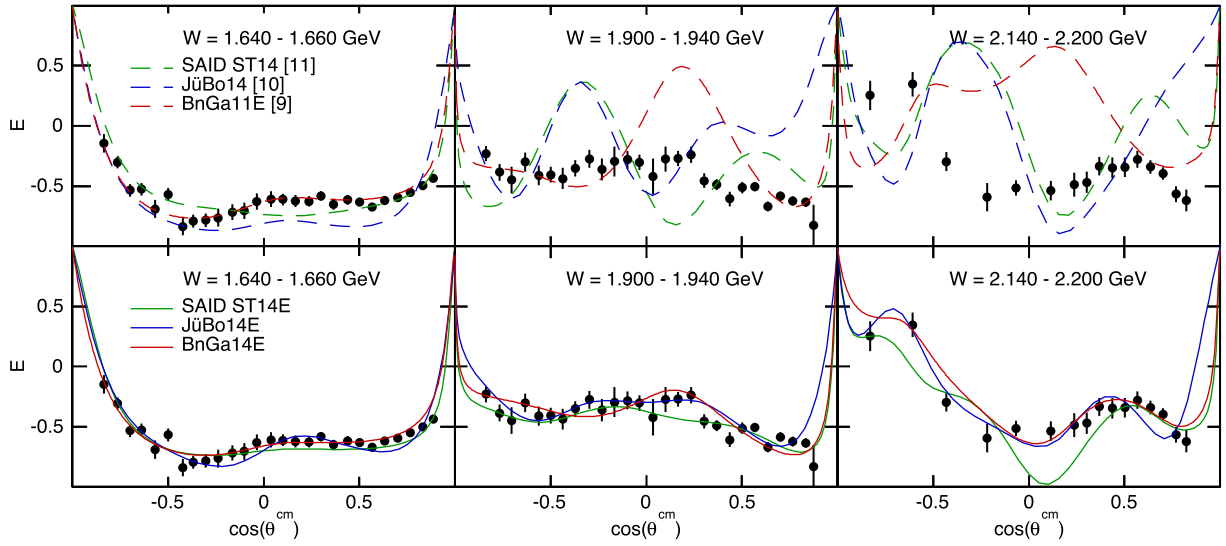

Fig. 3. (Color online.) Double polarization observable E in the $\vec{\gamma}\vec{p} \to \pi^+ n$ reaction as a function of $\cos\theta_\pi^{\rm cm}$ for three selected bins of the center-of-mass energy W. Systematic uncertainties are indicated as shaded bands. The curves in the upper panels are predictions based on the SAID ST14 [11] and JüBo14 [10] analyses as well as predictions from BnGa11E [9]. The curves in the lower panels are results from updated analyses including the present E data.

Table 1
Fits to the new CLAS data (labeled **E**) and previous results. Breit–Wigner helicity amplitudes for the SAID (ST14 based on CM12 [11]) and Bonn–Gatchina ([12]; †: entries from Ref. [9]) analyses. Values from Jülich–Bonn (JüBo14 based on Ref. [10]) are quoted at the T-matrix pole including the complex phase in parentheses. Helicity amplitudes $A_{1/2}$ and $A_{3/2}$ are given in units of $(\text{GeV})^{-1/2} \times 10^{-3}$.

		ST14	ST14**E**	JüBo14	JüBo14**E**	BnGa11E	BnGa14**E**
$N(1440)1/2^+$	$A_{1/2}$	-65 ± 5	-60 ± 5	$-56(+5°)$	$-53(-6°)$	-62 ± 8	-60 ± 8
$N(1520)3/2^-$	$A_{1/2}$	-22 ± 2	-24 ± 2	$-25(-13°)$	$-22(-14°)$	-20 ± 3	-24 ± 4
	$A_{3/2}$	142 ± 5	138 ± 3	$112(+28°)$	$104(+22°)$	131 ± 7	130 ± 6
$N(1535)1/2^-$	$A_{1/2}$	115 ± 10	120 ± 10	$52(-14°)$	$51(-20°)$	105 ± 9	100 ± 12
$N(1650)1/2^-$	$A_{1/2}$	55 ± 30	60 ± 30	$28(+7°)$	$30(-21°)$	33 ± 7	32 ± 6
$\Delta(1620)1/2^-$	$A_{1/2}$	35 ± 5	30 ± 5	$23(+14°)$	$25(+13°)$	52 ± 5	59 ± 8
$\Delta(1700)3/2^-$	$A_{1/2}$	128 ± 20	150 ± 20	$118(-6°)$	$121(-14°)$	$160 \pm 20^\dagger$	165 ± 20
	$A_{3/2}$	91 ± 30	110 ± 30	$106(+20°)$	$116(+52°)$	$165 \pm 25^\dagger$	170 ± 25
$\Delta(1905)5/2^+$	$A_{1/2}$	30 ± 6	30 ± 5	$13(+17°)$	$-39(+26°)$	$25 \pm 5^\dagger$	30 ± 8
	$A_{3/2}$	-70 ± 10	-50 ± 10	$-79(-59°)$	$-49(-67°)$	$-49 \pm 4^\dagger$	-50 ± 5
$\Delta(1950)7/2^+$	$A_{1/2}$	-70 ± 5	-80 ± 5	$-70(-15°)$	$-64(-16°)$	-70 ± 5	-68 ± 5
	$A_{3/2}$	-90 ± 5	-90 ± 5	$-86(-8°)$	$-91(-7°)$	-93 ± 5	-94 ± 4

the pole. While these quantities are different in principle, a recent study [24] has found qualitative agreement between the moduli of pole residues and real Breit–Wigner quantities. Comparisons between the two sets will be made at this qualitative level.

The SAID resonance couplings have changed only slightly for most states, usually within the estimated uncertainties of the extraction. As no new states are explicitly added, the fit below the highest energies has been accomplished with only small changes to the existing states. For the highest energies, unambiguous resonance extraction is complicated by a number of factors. Here, the non-resonant background is significant, as can be seen from the dominant forward peaking in the cross section [25]. In addition, one must deal with the interference of many amplitudes of a similar size, with resonances tending to be coupled only weakly to the πN channel.

The results given in Table 1 can be compared in detail with a similar table presented in the CBELSA-TAPS Collaboration analysis of E data for $\pi^0 p$ photoproduction [12]. Here the BnGa11E column gives the result of including these new $\pi^0 p$ E data in a fit. As the BnGa11E fit changed very little, these values (indicated with daggers) have been taken from the BnGa2011 solution [9]. Comparison with the fit ST14E is interesting in that almost all helicity amplitudes agree with those from BnGa11E, within quoted errors.

Including the new $E(\pi^0 p)$ data [12] in the JüBo14 analysis led to an improved description of the $E(\pi^+ n)$ data at intermediate energies but still failed to describe the new data at high energies (cf. Fig. 3). The impact of the new $E(\pi^+ n)$ data on some resonance parameters is significant in the JüBo14E re-analysis. For the $N(1650)1/2^-$ the phase changes by 28°, but also the SAID analysis finds that this helicity coupling is not well determined. The $N(1535)1/2^-$ helicity coupling is small because that resonance is narrower than in other analyses [10]. For some prominent resonances, such as the Roper, the $N(1520)3/2^-$, the $\Delta(1232)3/2^+$, and the $\Delta(1950)7/2^+$, the E data change the modulus and complex phase of the helicity couplings only moderately by around 10%. In contrast, for less prominent and more inelastic resonances, changes can be much larger as in case of the $\Delta(1905)5/2^+$. In the JüBo14E solution, changes in very high-L multipoles are larger than for the SAID analysis. Through correlations, high multipoles induce changes in lower multipoles. This explains why the new data has a larger impact for the Jülich–Bonn analysis than for the SAID analysis.

One poorly known state, the $\Delta(2200)\frac{7}{2}^-$, emerges and plays an important role in improving the Bonn–Gatchina fit at the highest energies.[4] This state also exists in the Jülich–Bonn analysis, but is not included in the SAID analysis. If this state exists, it would be in plain conflict with the prediction of models assuming a phase transition in high-mass resonances.

In summary, we have presented measurements of the double-polarization observable E in the $\vec{\gamma}\vec{p} \to \pi^+ n$ reaction up to $W = 2.3$ GeV over a large angular range. These results are the first of the FROST program at JLab. The fine binning and unprecedented quantity of the data impose tight constraints on partial-wave analysis, especially at high-L multipoles and at high center-of-mass energies where new resonances are expected to exist. These more tightly constrained amplitudes help to fix the πN components of larger multi-channel analyses as well. The SAID and Bonn–Gatchina solutions found minor changes of helicity couplings for most resonances, while the new E data led to major changes for the Jülich–Bonn solution and indications for a new state in the BnGa re-analysis.

[4] Details of this coupled-channel analysis are presented in a follow up paper.

Acknowledgements

The authors gratefully acknowledge the work of the Jefferson Lab staff. This work was supported by the U.S. National Science Foundation, the U.S. Department of Energy (DOE), the Chilean Comisión Nacional de Investigación Científica y Tecnológica (CONICYT), the Deutsche Forschungsgemeinschaft (SFB/TR16), the French Centre National de la Recherche Scientifique and Commissariat à l'Energie Atomique, the Italian Istituto Nazionale di Fisica Nucleare, JSC (JUROPA) at FZ Jülich, the National Research Foundation of Korea, the Russian Foundation of Fundamental Research, the Russian Science Foundation (RNF), and the UK Science and Technology Facilities Council (STFC). Jefferson Science Associates, LLC, operates the Thomas Jefferson National Accelerator Facility for the United States Department of Energy under contract DE-AC05-060R23177.

References

[1] V. Credé, W. Roberts, Rep. Prog. Phys. 76 (2013) 076301.
[2] E. Klempt, J.-M. Richard, Rev. Mod. Phys. 82 (2010) 1095.
[3] M. Anselmino, E. Predazzi, S. Ekelin, S. Fredriksson, D. Lichtenberg, Rev. Mod. Phys. 65 (1993) 1199.
[4] S.J. Brodsky, Eur. Phys. J. A 31 (2007) 638.
[5] E. Kolomeitsev, M. Lutz, Phys. Lett. B 585 (2004) 243.
[6] S. Afonin, Int. J. Mod. Phys. A 22 (2007) 4537.
[7] W.-T. Chiang, F. Tabakin, Phys. Rev. C 55 (1997) 2054.
[8] I.S. Barker, A. Donnachie, J.K. Storrow, Nucl. Phys. B 95 (1975) 347.
[9] A. Anisovich, et al., Eur. Phys. J. A 48 (2012) 15.
[10] Rönchen, et al., Eur. Phys. J. A 50 (2014) 101.
[11] R.L. Workman, M.W. Paris, W.J. Briscoe, I.I. Strakovsky, Phys. Rev. C 86 (2012) 015202.
[12] M. Gottschall, et al., Phys. Rev. Lett. 112 (2014) 012003.
[13] J. Ahrens, et al., Phys. Rev. Lett. 88 (2002) 232002.
[14] J. Ahrens, et al., Eur. Phys. J. A 21 (2004) 323.

[15] J. Ahrens, et al., Phys. Rev. C 74 (2006) 045204.
[16] D. Sober, et al., Nucl. Instrum. Methods A 440 (2000) 263.
[17] H. Olsen, L.C. Maximon, Phys. Rev. 114 (1959) 887.
[18] C. Keith, J. Brock, C. Carlin, S. Comer, D. Kashy, J. McAndrew, D. Meekins, E. Pasyuk, J. Pierce, M. Seely, Nucl. Instrum. Methods A 684 (2012) 27.
[19] B.A. Mecking, et al., Nucl. Instrum. Methods A 503 (2003) 513.
[20] Y. Sharabian, et al., Nucl. Instrum. Methods A 556 (2006) 246.
[21] M. Mestayer, et al., Nucl. Instrum. Methods A 449 (2000) 81.
[22] E. Smith, et al., Nucl. Instrum. Methods A 432 (1999) 265.
[23] D. Drechsel, S. Kamalov, L. Tiator, Eur. Phys. J. A 34 (2007) 69.
[24] R.L. Workman, L. Tiator, A. Sarantsev, Phys. Rev. C 87 (2013) 068201.
[25] G. Buschhorn, et al., Phys. Rev. Lett. 18 (1967) 571.